The Plant Cell, Vol. 27: 2501–2515, September 2015, www.plantcell.org

Aluminum-Dependent Terminal Differentiation of the Arabidopsis Root Tip Is Mediated through an ATR-, ALT2-, and SOG1-Regulated Transcriptional Response[OPEN]

Caroline A. Sjogren, Stephen C. Bolaris, and Paul B. Larsen[1]

Department of Biochemistry, University of California, Riverside, California 92521

ORCID ID: 0000-0002-6992-9067 (P.B.L.)

By screening for suppressors of the aluminum (Al) hypersensitive *Arabidopsis thaliana* mutant *als3-1*, it was found that mutational loss of the Arabidopsis DNA damage response transcription factor *SUPPRESSOR OF GAMMA RESPONSE1* (*SOG1*) confers increased Al tolerance similar to the loss-of-function mutants for the cell cycle checkpoint genes *ATAXIA TELANGIECTASIA AND RAD3 RELATED* (*ATR*) and *ALUMINUM TOLERANT2* (*ALT2*). This suggests that Al-dependent terminal differentiation of the root tip is an active process resulting from activation of the DNA damage checkpoint by an ATR-regulated pathway, which functions at least in part through SOG1. Consistent with this, ATR can phosphorylate SOG1 in vitro. Analysis of SOG1's role in Al-dependent root growth inhibition shows that *sog1-7* prevents Al-dependent quiescent center differentiation and endoreduplication in the primary root tip. Following Al exposure, SOG1 increases expression of several genes previously associated with DNA damage, including *BRCA1* and *PARP2*, with gel-shift analysis showing that SOG1 can physically associate with the *BRCA1* promoter in vitro. Al-responsive expression of these SOG1-regulated genes requires ATR and ALT2, but not ATAXIA TELANGIECTASIA MUTATED, thus demonstrating that in response to chronic Al exposure, ATR, ALT2, and SOG1 function together to halt root growth and promote terminal differentiation at least in part in a transcription-dependent manner.

INTRODUCTION

Aluminum (Al) toxicity is a global agricultural problem that results in severe root growth inhibition in acidic soil environments, which comprise >30% of the world's arable land (von Uexkull and Mutert, 1995). Two distinctly different types of mechanisms have been described that allow plants to cope with Al in their environment. These include resistance mechanisms that depend on exclusion of Al from plant tissues and tolerance mechanisms that increase the plant's capability to withstand the toxic effects of Al accumulation within its tissues (Kochian, 1995). Significant progress has been made in development of an understanding of how plants prevent internalization of Al, particularly in determining the mechanisms by which plant roots secrete organic acids that can chelate Al, following exposure to Al (Sasaki et al., 2004; Hoekenga et al., 2006). Such Al resistance mechanisms have largely been described in agriculturally relevant plants such as maize (*Zea mays*), wheat (*Triticum aestivum*), and sorghum (*Sorghum bicolor*). Based on the significant biodiversity in acid soil regions, increased Al tolerance likely also is an important strategy to allow native plants to thrive in environments that would normally be inhibitory to plant species not adapted to acid soils.

Developing an understanding of the mechanisms of Al tolerance has been considered to be intractable, due to the predicted multitude of inter- and intracellular targets for Al^{3+}. This is largely because Al^{3+}, the toxic form of Al that predominates at low pH, can competitively displace biologically relevant cations, such as Mg^{2+}, and disrupt the activities of enzymes that depend on these cations to function (Macdonald and Martin, 1988). Since cations are also important for conformation and function of large anionic macromolecules such as DNA, it has been argued that nucleic acids are a direct target of Al^{3+} in biological systems, potentially through interactions with the negative charges on the phosphodiester backbone (Karlik et al., 1980). Consequently, due to the predicted complexity of Al toxicity following internalization, it has been hard to envisage that single changes in biochemical targets could result in a measurable increase in Al tolerance.

To develop an understanding of how Al affects cellular function and to identify factors that participate in Al tolerance, a mutagenesis approach was previously undertaken that resulted in identification of *Arabidopsis thaliana* mutants with hypersensitivity to Al. This work identified eight complementation groups that affected-factors predicted to be required for detoxification of Al following internalization, including *als1-1* and *als3-1* (Larsen et al., 1997, 2005, 2007). Both mutations negatively impact factors that had features of transporters and were speculated to act in redistribution of Al away from sensitive areas of the root. Most striking was the severity of the phenotype of *als3-1* in the presence of levels of $AlCl_3$ that had no discernible effect on root growth of wild-type Arabidopsis.

ALS3 encodes a factor related to ABC transporters (Larsen et al., 2005) that is localized to the plasma membrane of cells of the root tip and vasculature and is predicted to be required for redistribution of Al away from highly sensitive tissues. In support of this, mutational loss of *ALS3* results in extreme Al hypersensitivity, with *als3-1* roots being severely inhibited by long-term chronic exposure to as little as 10 to 20 μM $AlCl_3$ in

[1] Address correspondence to paul.larsen@ucr.edu.
The author responsible for distribution of materials integral to the findings presented in this article in accordance with the policy described in the Instructions for Authors (www.plantcell.org) is: Paul B. Larsen (paul.larsen@ucr.edu).
[OPEN]Articles can be viewed online without a subscription.
www.plantcell.org/cgi/doi/10.1105/tpc.15.00172

a hydroponic environment (pH 4.2), although this level has no measurable effect on Col-0 wild-type roots in the complex nutrient media that is used for hydroponic studies (Larsen et al., 1997). In association with the Al hypersensitivity of *als3-1*, roots of the mutant demonstrate terminal differentiation at these subthreshold levels of Al, which is suggestive of Al not being properly removed from the root tip and triggering a programmatic response that halts cell division and promotes endocycling (e.g., Figure 3C) (Rounds and Larsen, 2008). Consequently, because of its extreme response to normally noninhibitory levels of Al, *als3-1* represented a valuable opportunity to identify suppressors that restore root growth of the mutant in the presence of Al as a means to define both Al tolerance mechanisms and paramount sites of Al toxicity (Gabrielson et al., 2006).

Screening for *als3-1* suppressors showed that DNA damage checkpoints play a critical role in stoppage of root growth following chronic exposure to Al. Currently, two separate *als3-1* suppressor mutations have been reported including mutations that affect genes encoding a key cell cycle checkpoint regulator, ATAXIA TELANGIECTASIA AND RAD3 RELATED (ATR) (Rounds and Larsen, 2008), and a WD-40 protein, ALUMINUM TOLERANT2 (ALT2) (Nezames et al., 2012), both of which participate in surveillance of DNA integrity. ATR, a kinase universally found in eukaryotes, plays a key role in monitoring for DNA damage (Culligan et al., 2004). ATR is closely related to ATAXIA TELANGIECTASIA MUTATED (ATM), but each has a distinctively different role in assessing DNA damage (Culligan et al., 2006). Whereas ATM responds to DNA damage in the form of double strand breaks, ATR is activated by persistent single stranded DNA resulting from genotoxic agents that cause replication forks to stall. The participation of ATR in actively halting root growth following Al exposure strongly suggests that Al is perceived as a genotoxin, albeit in a currently unknown manner (Rounds and Larsen, 2008). It is particularly striking that while loss-of-function mutations in *ATR* and *ALT2* result in severe hypersensitivity to various DNA damage agents such as DNA cross-linkers, this is not the case for Al toxicity since loss of either of these factors results in measurable increases in Al tolerance even in comparison to the wild type. Consequently, it is currently unclear why Al activates this ATR-dependent DNA damage checkpoint pathway.

Previous work has shown that Arabidopsis ATM functions in conjunction with a NAC family transcription factor, SOG1, to increase expression of a suite of DNA damage response genes following accumulation of double strand breaks resulting from exposure to γ-radiation (Yoshiyama et al., 2009, 2013). SOG1 is a key determinant in transition from an actively dividing cell to one that undergoes endoreduplication, which arises from DNA replication in the absence of cytokinesis and results in terminal differentiation of the root tip and accumulation of cells with increased ploidy levels (Yoshiyama et al., 2013). As part of our ongoing attempt to identify suppressors of *als3-1* and to further our understanding of mechanisms of Al toxicity and tolerance, we found that a loss-of-function *sog1* mutant suppresses the severe hypersensitivity of *als3-1* in a manner similar to both *atr* and *alt2* loss-of-function mutants. Our results indicate that SOG1 participates in the ATR- and ALT2-regulated pathway in an ATM-independent manner to halt root growth actively and promote terminal differentiation following Al exposure.

RESULTS

Isolation and Characterization of an *als3-1* Suppressor Mutant

In order to understand further how Al actively promotes terminal differentiation, seeds of *als3-1* were mutagenized with ethyl methanesulfonate and M2 seedlings were screened for those with roots capable of sustained growth in the presence of 0.75 mM $AlCl_3$ (pH 4.2) in a soaked gel environment. Identified seedlings were rescued and allowed to set seeds, after which progeny were rescreened to identify bona fide *als3-1* suppressors. From this screen, we chose an *als3-1* suppressor mutant that was capable of sustained root growth in comparison to *als3-1* in the presence of a range of $AlCl_3$ concentrations (Figures 1A and 1B) for further analysis. Subsequent work (see below) showed this mutant to be an allele of *SUPPRESSOR OF GAMMA RESPONSE1* (*SOG1*); therefore, we refer to this suppressor as *sog1-7*.

To determine whether the *als3-1* suppression in the *sog1-7 als3-1*double mutants resulted from increased Al resistance or tolerance, a variety of physiological tests were conducted. Internalization of Al has been associated with deposition of the polysaccharide callose in the root tip (Horst et al., 1997). Seedlings of Col-0 wild type, *als3-1* single mutants, and the *sog1-7 als3-1* double mutants were grown hydroponically for 6 d and then exposed to either 0 or 25 μM $AlCl_3$ (pH 4.2), which is a concentration that causes moderate inhibition of wild-type root growth in our growth conditions, for 24 h. After these treatments, the seedlings were stained with Aniline blue to detect callose. Consistent with the *sog1-7 als3-1* plants having enhanced tolerance to internalized Al, their roots accumulated callose similarly to both Col-0 wild type and *als3-1* (Figure 1C). This suggests that even though callose accumulation is correlated with Al toxicity and has been suggested to be integral to Al dependent stoppage of root growth, it may not directly be related to growth inhibition (Horst et al., 2010).

It was also tested whether the *sog1-7 als3-1* plants showed Al-responsive increases in gene expression, as would be expected for enhanced Al tolerance rather than increased Al exclusion. For this experiment, seedlings of Col-0 wild type, *als3-1*, and the *sog1-7 als3-1* mutant were grown hydroponically for 6 d, after which seedlings were exposed to 0 or 25 μM $AlCl_3$ for 24 h. Following this, roots were collected and total RNA was isolated for RNA gel blot analysis with the Al-inducible probes *ALS3* and *ALMT1* (Larsen et al., 2005; Hoekenga et al., 2006). As shown in Figure 1D, exposure of Col-0 wild type, *als3-1*, and *sog1-7 als3-1* mutants to Al resulted in increased expression of both Al-responsive genes, thus indicating that the *als3-1* suppressor internalizes Al similarly to Col-0 wild type and *als3-1*.

Finally, total Al that accumulated in the root tissue of Col-0 wild type, *als3-1*, and the *sog1-7 als3-1* double mutant was measured using inductively coupled plasma-optical emission spectrometry (ICP-OES). For this experiment, seedlings were grown hydroponically for 6 d in the absence of Al, after which roots were exposed to 0 or 50 μM $AlCl_3$ for 24 h. Root tips were subsequently harvested, washed with nutrient medium, dried, and then ashed in pure HNO_3 in preparation for analysis. As shown in Figure 1E, all Al-treated root samples, including those of the *sog1-7 als3-1* mutant, showed significant accumulation of Al, thus

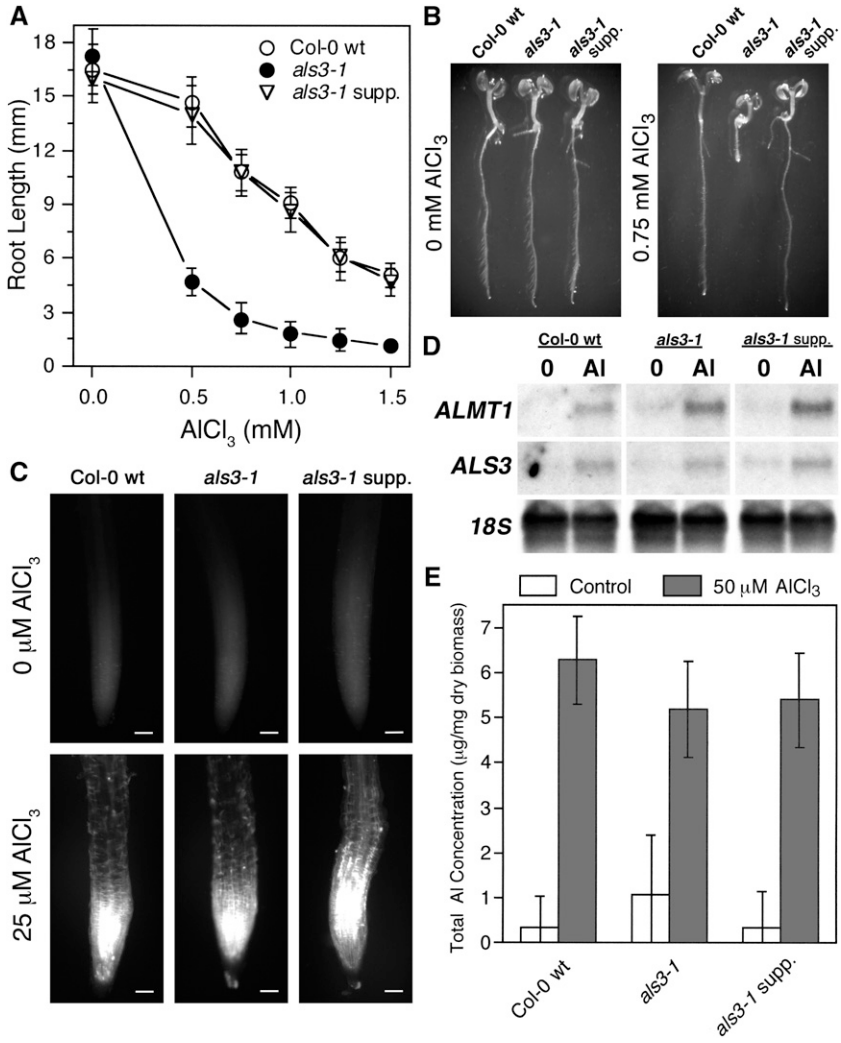

Figure 1. Growth Characterization of an *als3-1* Suppressor Mutant in the Presence of Al.

(A) and **(B)** Col-0 wild type, *als3-1*, and the *als3-1* line carrying the suppressor mutant *sog1-7* were grown in a soaked gel environment (pH 4.2) with either no or increasing concentrations of $AlCl_3$ (pH 4.2) for 7 d, after which root length was measured. Mean ± SD values were determined from 30 seedlings.
(C) Seedlings of Col-0 wild type, *als3-1*, and *sog1-7 als3-1* were grown for 6 d, after which they were exposed to either 0 or 25 μM $AlCl_3$ (pH 4.2) in hydroponics for 24 h and stained with Aniline blue for callose deposition. Seedlings were visualized using fluorescence microscopy. Bars = 50 μm.
(D) Seedlings of Col-0 wild type, *als3-1*, and *sog1-7 als3-1* were grown for 6 d, after which they were exposed to either 0 or 25 μM $AlCl_3$ (pH 4.2) in hydroponics for 24 h. Root tissue was harvested and total RNA was extracted for RNA gel blot analysis with Al-inducible genes.
(E) Col-0 wild-type, *als3-1*, and *sog1-7 als3-1* seedlings were grown for 6 d and then exposed for 24 h to either 0 or 50 μM $AlCl_3$ (pH 4.2) in hydroponics. Root tips were washed in nutrient medium without $AlCl_3$, harvested, dried, and ashed in nitric acid, and total Al content was measured using ICP-OES. Mean ± SD values were determined from five samples.

indicating that the observed restoration of root growth for the *sog1-7 als3-1* mutant was dependent on enhanced Al tolerance rather than reduced Al accumulation within the root tip.

A Loss-of-Function Mutation in *SOG1* Suppresses Al Hypersensitivity in *als3-1*

To identify the nature of the *als3-1* suppressor mutation, we used a map-based cloning approach. For this exercise, the *als3-1* line carrying the suppressor mutant (in the Col-0 background) was crossed to an *als3-1* line that had been introgressed into the La-0 background (Gabrielson et al., 2006). Because of the recessive nature of the *als3-1* suppressor mutation, F2 progeny from the cross were grown on gel plates soaked with 0.75 mM $AlCl_3$ (pH 4.2), and seedlings with roots that were capable of sustained growth were rescued. Following isolation of genomic DNA, PCR-based analyses were conducted and showed that the *als3-1* suppressor mutation localized to the top arm of Arabidopsis chromosome 1 (Figure 2A). Fine mapping resulted in a genetic window that allowed identification of candidate genes for sequence analysis. The *als3-1* suppressor mutation was subsequently found to be in exon 4 of *At1g25580*, which was

previously reported as the ATM-regulated transcription factor *SOG1* that is responsible for initiation of endoreduplication following exposure to DNA damage agents (Yoshiyama et al., 2009). The *als3-1* suppressor mutation represents an amino acid substitution (S206F) in the predicted NAC domain of this NAM (no apical meristem), ATAF1/ATAF2, CUC (cup-shaped cotyledon) (NAC) family transcription factor (Figure 2B).

Functional complementation was subsequently performed using a full-length genomic *SOG1* construct that was previously reported (Yoshiyama et al., 2009). Seedlings of Col-0 wild type, *als3-1*, *sog1-7 als3-1*, and *sog1-7 als3-1* carrying a wild-type genomic version of *SOG1* were grown in the presence of 0.75 mM $AlCl_3$ (pH 4.2) in a soaked gel environment for 7 d, after which seedling roots were assessed for terminal differentiation. As shown in Figure 2C, introduction of a wild-type genomic version of *SOG1* into *sog1-7 als3-1* fully restored Al hypersensitivity to *sog1-7 als3-1*, as demonstrated by the transgenic root being terminally differentiated in a manner indistinguishable from Al-treated *als3-1*.

We also tested whether another loss-of-function allele of *SOG1*, *sog1-1* (SOG^{R155G}), could suppress the *als3-1* phenotype (Yoshiyama et al., 2009). For this analysis, a *sog1-1 als3-1* mutant was generated and its capability to grow in an Al toxic environment was compared with Col-0 wild type, *als3-1*, and *sog1-7 als3-1*. As shown in Figure 2D, seedlings were grown for 7 d in the presence of 0.75 mM $AlCl_3$ (pH 4.2) in a soaked gel environment, after which root tips were assessed for terminal differentiation. This showed that the *sog1-1* allele can suppress the extreme Al response of *als3-1* in a manner indistinguishable from *sog1-7* since both *sog1-1 als3-1* and *sog1-7 als3-1* failed to exhibit the severe root growth inhibition seen for Al-treated *als3-1*.

It was subsequently determined how well *sog1-7* roots grew without the *als3-1* mutation in the background. For this analysis, *sog1-7* was backcrossed to Col-0 wild type, and homozygous *sog1-7* progeny were identified by PCR analysis. Col-0 wild-type and *sog1-7* seedlings were then grown for 7 d in the absence or presence of increasing concentrations of $AlCl_3$ (pH 4.2) in a soaked gel environment, after which root lengths were measured. As shown in Figure 2E, in the absence of *als3-1*, the *sog1-7* mutant roots showed greater growth than wild-type roots in the presence of a range of normally highly inhibitory levels of $AlCl_3$, thus indicating that SOG1 has a prominent role in actively halting root growth following Al treatment.

Real-time PCR analysis was performed to determine if *SOG1* expression is regulated by Al. Col-0 wild-type and *sog1-7* seedlings were grown in a hydroponic environment for 6 d after which they were treated with 0, 25, or 100 μM $AlCl_3$ (pH 4.2) for 24 h. Root tissue was collected and total RNA was isolated for cDNA synthesis and RT-PCR. As shown in Figure 2F, there was no indication that *SOG1* is transcriptionally induced by Al nor was it found that the *sog1-7* mutation affects transcript stability since Col-0 wild type and *sog1-7* showed comparable levels of *SOG1* transcript.

SOG1 Causes Terminal Differentiation in Response to Al

Mutational loss of the cell cycle checkpoint factors *ATR* and *ALT2* results in increased root growth in the presence of Al that is correlated with failure to halt cell cycle progression in conjunction with forced quiescent center (QC) differentiation (Rounds and Larsen, 2008; Nezames et al., 2012). In order to determine if this is also the case for roots of a *sog1* loss-of-function mutant, *sog1-7* was crossed to either a transgenic Arabidopsis line carrying a reporter for cell cycle progression, *CYCB1;1:GUS* (Colón-Carmona et al., 1999), or a reporter for QC status, *QC46* (Sabatini et al., 2003). Seedlings of Col-0 wild type and *sog1-7* carrying the *CYCB1;1:GUS* reporter were grown in the absence or presence of 0.75 mM $AlCl_3$ (pH 4.2) in a soaked gel environment for 7 d, after which they were stained for GUS activity. As shown in Figure 3A, treatment of Col-0 wild type carrying the *CYCB1;1:GUS* reporter results in a substantial increase in GUS activity following exposure to Al, which is consistent with a large number of root cells being incapable of exiting the G2 phase of mitosis and proceed into actual cell division. Unlike previous reports for the *atr-4* and *alt2-1* loss-of-function mutations (Rounds and Larsen, 2008; Nezames et al., 2012), introgression of this reporter into the *sog1-7* background did not eliminate Al-dependent CYCB1;1 accumulation, although the levels of the CYCB1;1:GUS reporter were substantially reduced in Al-treated *sog1-7* roots compared with Col-0 wild type. This suggests that while SOG1 likely contributes to Al-dependent inhibition of cell cycle progression at the G2 phase, ATR and ALT2 likely also function through other factors to prevent CYCB1;1 turnover.

Consistent with prior results, it was found that Al treatment results in loss of the QC as measured by *QC46* dependent GUS activity that is localized to the root stem cells (Rounds and Larsen, 2008; Nezames et al., 2012). For this analysis, *QC46* transgenic seedlings in either the Col-0 wild type or *sog1-7* backgrounds were grown for 7 d in the absence or presence of 1.50 mM $AlCl_3$ (pH 4.2) in a soaked gel environment, after which seedlings were stained to visualize the QC. As shown in Figure 3B, both Col-0 wild-type and *sog1-7* roots had a discernible QC in the absence of Al. Treatment with high levels of Al resulted in loss of the QC in Col-0 wild type but not *sog1-7*, thus indicating that SOG1 plays an active role in differentiation of the QC following Al treatment likely as a step in the transition to endoreduplication in the root tip.

In support of this model, it was found that Al treatment leads to terminal differentiation in conjunction with substantial increases in cell and nucleus size in *als3-1* roots. For this analysis, Col-0 wild-type, *als3-1*, *atr-4 als3-1*, *alt2-1 als3-1*, and *sog1-7 als3-1* plants were grown in the absence or presence of 0.75 mM $AlCl_3$ (pH 4.2) in a soaked gel environment, after which seedlings were fixed and stained with 4′,6-diamidino-2-phenylindole (DAPI). Root tips were subsequently visualized using confocal microscopy at the same magnification for each. As shown in Figure 3C, Al treatment results in substantial increases in both cell and nuclear size for *als3-1* roots, which is consistent with terminal differentiation in conjunction with endoreduplication. In contrast, *atr-4 als3-1*, *alt2-1 als3-1*, and *sog1-7 als3-1* roots did not show the dramatic Al-dependent increases in cell and nuclear size as seen for Al-treated *als3-1* roots, thus indicating that all three suppressor mutants block the Al hypersensitivity of *als3-1* in conjunction with prevention of terminal differentiation and endoreduplication.

ATR and SOG1 Likely Function Together to Promote Al-Dependent Stoppage of Root Growth

Since loss-of-function mutants for *SOG1* and *ATR* are phenotypically similar with regard to Al tolerance (Rounds and Larsen, 2008; e.g., Figure 3C), it might be expected that these two cell

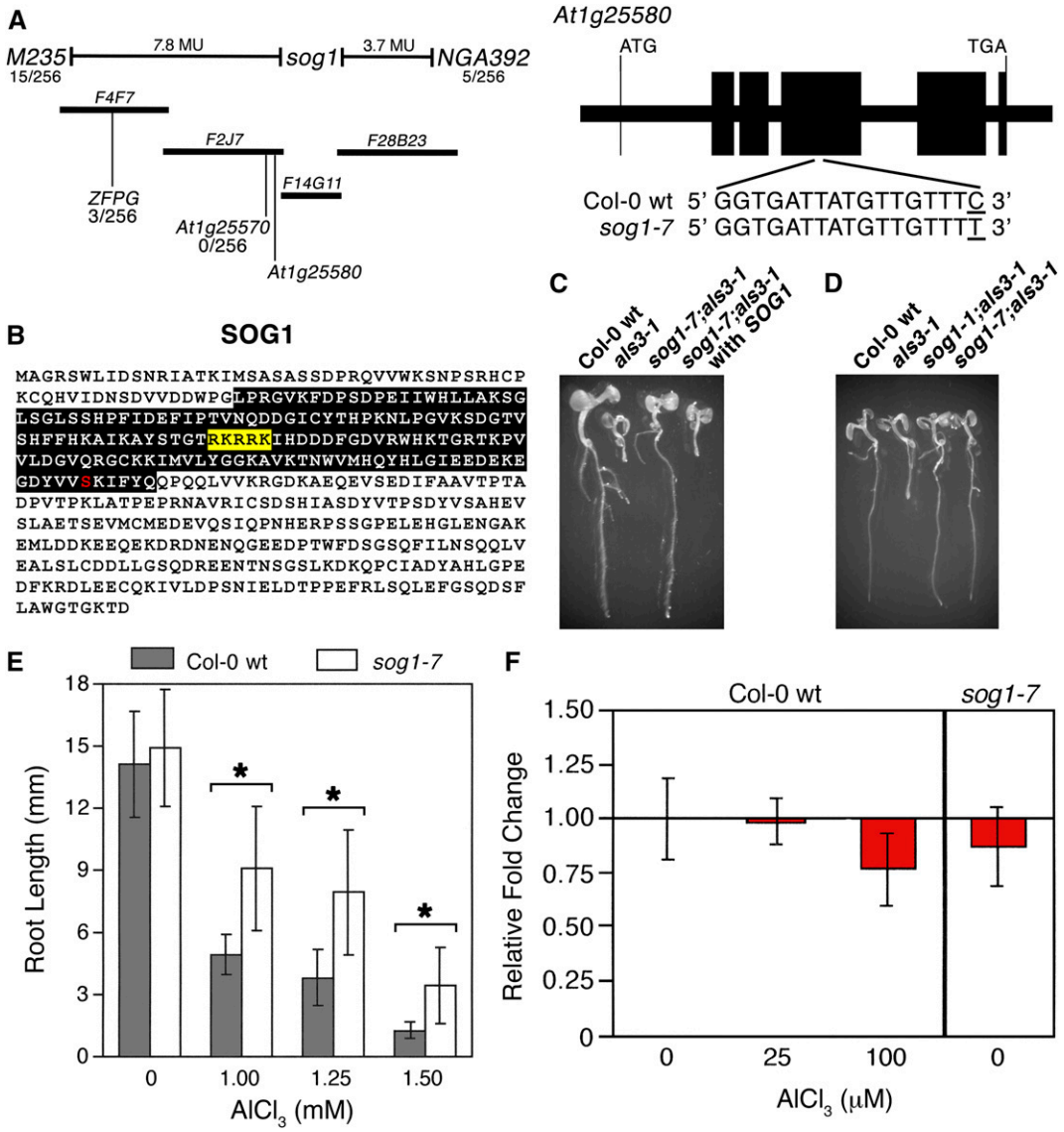

Figure 2. Loss of *SOG1* Results in Suppression of Al Hypersensitivity in *als3-1*.

(A) Map-based cloning of the *als3-1* suppressor (Col-0 background) crossed to *als3-1* (Ws background) localized the second site mutation to the top arm of chromosome 1. Sequencing of candidates in the genetic window revealed a single nucleotide change in exon 4 of *At1g25580*, also known as *SOG1*.
(B) Amino acid sequence of SOG1, showing the predicted NAC domain of the transcription factor (black box), the predicted nuclear localization signal (yellow box), and the effect of the nucleotide change in *sog1-7* on primary structure (S206F).
(C) Introduction of wild-type *SOG1*, including promoter, all exons and introns, and 5′ and 3′ untranslated regions, restores Al hypersensitivity to *sog1-7 als3-1* grown for 7 d in the presence of 0.75 mM $AlCl_3$ (pH 4.2) in a soaked gel environment.
(D) The *sog1-1* allele suppresses the Al hypersensitivity phenotype of *als3-1* as shown by growth of *sog1-1;als3-1* for 7 d in the presence of 0.75 mM $AlCl_3$ (pH 4.2) in a soaked gel environment.
(E) Growth of *sog1-7* and Col-0 wild type for 7 d in the absence or presence of increasing concentrations of $AlCl_3$ in a soaked gel environment shows that *sog1-7* roots are more Al tolerant than Col-0 wild type. Mean ± SD values were determined from 30 seedlings. Asterisk indicates significance at $P \leq 0.01$ when comparing Al-treated lines using the Kruskal-Wallis one-way ANOVA test.
(F) *SOG1* transcript levels in Col-0 wild type, in the absence or presence of $AlCl_3$, and in *sog1-7* were determined by real-time PCR using mRNA isolated from root tissue. Seedlings were grown for 6 d in a hydroponic environment, after which they were transferred to 0, 25, or 100 μM $AlCl_3$ (pH 4.2) for 24 h.

cycle checkpoint factors act together to trigger Al-dependent terminal differentiation of the root. In order to test whether there is a relationship between these two factors in Al-dependent stoppage of root growth, a *sog1-7 atr-4* mutant was generated and tested for its capability to grow in the presence of Al. For this experiment, Col-0 wild type, *sog1-7*, *atr-4*, and *sog1-7 atr-4* were grown for 7 d in the absence or presence of 1.50 mM $AlCl_3$ (pH 4.2) in a soaked gel environment, after which root lengths were

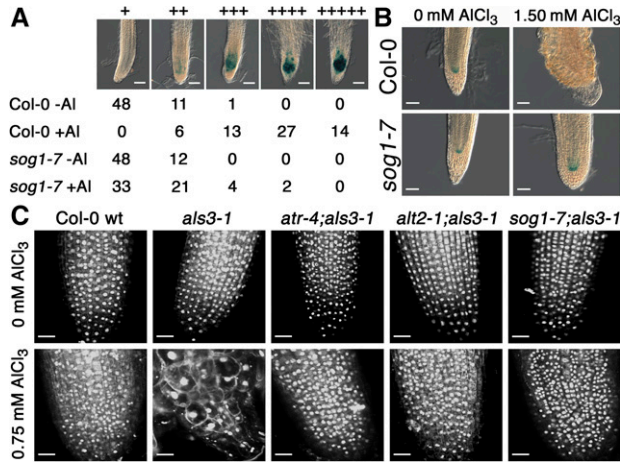

Figure 3. Loss of *SOG1* Function Prevents Terminal Differentiation and Blocks Al-Dependent Endoreduplication in *als3-1*.

(A) Seedlings of Col-0 wild type and *sog1-7*, each of which carried the CDS of *CyclinB1;1* including a predicted mitotic destruction box fused to the *GUS* reporter, were grown for 7 d in the absence or presence of 0.75 mM $AlCl_3$ (pH 4.2) in a soaked gel environment, after which seedlings were stained for 1 h for GUS activity and primary root tips were scored for blue color (1 = no color and 5 = intense blue color). Bars = 50 μm.
(B) Seedlings of Col-0 wild type and *sog1-7*, both of which carried the GUS-based *QC46* marker for the quiescent center, were grown for 7 d in the absence or presence of 1.50 mM $AlCl_3$ (pH 4.2) in a soaked gel environment, after which seedlings were stained for GUS activity for 24 h. Bars = 50 μM.
(C) Seedlings of Col-0 wild type, *als3-1*, *atr-4 als3-1*, *alt2-1 als3-1*, and *sog1-7 als3-1* were grown for 7 d in the absence or presence of 0.75 mM $AlCl_3$ (pH 4.2) in a soaked gel environment, after which samples were fixed in FAA and stained with DAPI. Root tips were visualized at 40× magnification via confocal microscopy for both cell and nucleus size. Bars = 25 μm.

measured. As shown in Figure 4A, the *sog1-7 atr-4* mutant was comparable to *sog1-7* and *atr-4* for Al tolerance, thus suggesting that SOG1 and ATR are part of the same pathway that halts root growth following exposure to Al.

Al-Dependent Terminal Differentiation Is Linked to Loss of *SOG1* Expression

Because SOG1 has been linked to stoppage of root growth following Al treatment and Al toxicity is most pronounced at the root tip (Ryan et al., 1993), it was of interest to determine the tissue localization pattern for SOG1. For this analysis, a previously reported transgenic Arabidopsis line carrying a *SOG1:GUS* fusion construct (−1840 to +3794) (Yoshiyama et al., 2013) was grown in the absence or presence of 1.50 mM $AlCl_3$ (pH 4.2) in a soaked gel environment for 7 d, after which seedlings were stained for GUS activity. As shown in Figure 4B, consistent with the role of SOG1 in promoting terminal differentiation of the root tip following Al exposure, GUS activity was clearly observed throughout the root tip. In contrast, root tips treated with Al for 7 d showed no GUS activity, thus indicating that SOG1 does not persist after a root has terminally differentiated following Al treatment. Loss of *SOG1* expression in the presence of inhibitory levels of Al is apparently ATR-dependent since SOG1:GUS is maintained in root tips of the loss-of-function *atr-4* mutant even following Al treatment. It should be noted that even though severely compromised, the terminal differentiation seen for Al-treated roots is not associated with tissue death as shown by Evan's blue staining in previous studies (Rounds and Larsen, 2008; Nezames et al., 2012).

SOG1 Can Be Phosphorylated by ATR in Vitro

Since there is an apparent functional relationship between ATR and SOG1 with regard to terminal differentiation of the root tip following Al exposure, it was of interest to determine whether SOG1 is a phosphorylation target of ATR. For this analysis, the entire coding sequence (CDS) of Arabidopsis *ATR* representing 2702 amino acids was produced as a GST fusion protein in a baculovirus protein expression system. In conjunction with this, the entire CDS of Arabidopsis *SOG1*, representing 449 amino acids, was produced as a Maltose Binding Protein (MBP) fusion in an *Escherichia coli* BL21-DE3 *pLysS* protein expression system. Approximately 50 ng of GST-ATR was subsequently incubated with 1 μg of either MBP or MBP-SOG1 in the presence of [γ-^{32}P] ATP, after which samples were separated on an SDS-PAGE gel, which was visualized by autoradiography. As shown in Figure 4C, incubation of MBP with GST-ATR did not result in measurable phosphorylation of MBP. In contrast, incubation of MBP-SOG1 with GST-ATR resulted in a distinct radiolabeled band that was the same size as that predicted for MBP-SOG1, thus indicating that at least in vitro, SOG1 is a phosphorylation target of the Arabidopsis ATR kinase.

SOG1 Binds to the *BRCA1* Promoter in Vitro

SOG1, which is a member of the NAC family of transcription factors, can bind directly to DNA (Yi et al., 2014). Additionally, *BRCA1* expression increased following exposure to γ-radiation, in a SOG1-dependent manner (Yoshiyama et al., 2009), suggesting that *BRCA1* expression may be directly dependent on SOG1 binding to the *BRCA1* promoter. In order to test this, bacterially produced MBP-SOG1 was used for an electrophoretic mobility shift assays (EMSAs) with the *BRCA1* promoter (−1500 to −1). As shown in Figure 4D, incubation of MBP alone with the *BRCA1* promoter resulted in no detectable change in migration of the radiolabeled DNA. In contrast, addition of 50 ng of MBP-SOG1^{wt} caused a discernible shift in the migration of the *BRCA1* promoter fragment, consistent with a physical interaction. In support of this, addition of increasing concentrations of unlabeled *BRCA1* promoter resulted in a severe reduction in the observed SOG1-dependent shift of the *BRCA1* promoter, thus indicating that SOG1 is capable of physically associating with promoters of the suite of genes that are expressed in a SOG1-dependent manner.

Two different loss-of-function *sog1* mutations have now been described, including *sog1-1* (SOG1^{R155G}) and *sog1-7* (SOG1^{S206F}). Consequently, it was of interest to determine whether either mutation would impact the capability of MBP-SOG1 to bind to the *BRCA1* promoter in this EMSA assay. As shown in Figure 4D, introduction of either of the mutations severely reduced or abolished binding of MBP-SOG1 to the *BRCA1* promoter, thus suggesting that each mutation leads to the described loss-of-function phenotypes at least in part due to loss

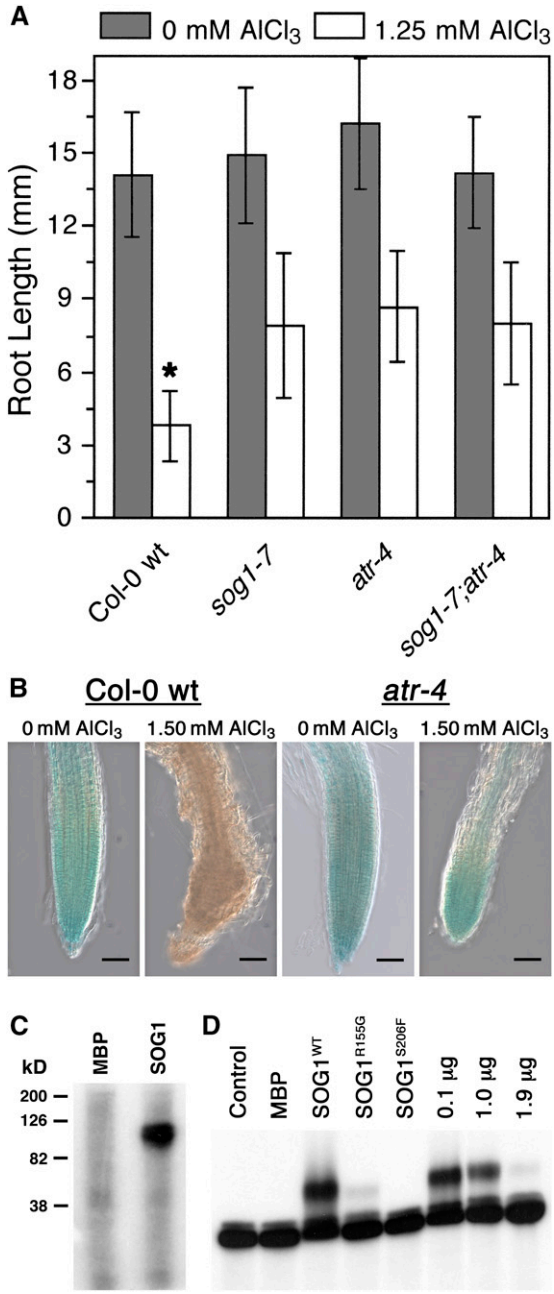

Figure 4. SOG1 Works in Conjunction with ATR to Promote Al-Dependent Stoppage of Root Growth.

(A) A *sog1-7 atr-4* double mutant was grown for 7 d in the absence or presence of 1.25 mM $AlCl_3$ (pH 4.2) in a soaked gel environment in order to determine whether the combination of mutations is additive for Al tolerance. Mean ± SD values were determined from 30 seedlings. Asterisk indicates significance at $P \leq 0.01$ when comparing Al-treated lines using the Tukey HSD test.

(B) *SOG1* expression was found to be localized in part to the Arabidopsis root tip using a *SOG1:GUS* transgenic line grown for 7 d in either the absence or presence of 1.50 mM $AlCl_3$ (pH 4.2) in a soaked gel environment, after which seedlings were stained for GUS activity for 1 h. Al treatment resulted in loss of SOG1:GUS in Col-0 wild type but not in an *atr* loss-of-function mutant, indicating that Al-dependent changes in SOG1 levels are regulated by ATR likely as a part of ATR-dependent terminal differentiation. Bars = 50 μm.

(C) Full-length Arabidopsis ATR protein was produced using a baculovirus protein expression system. Approximately 100 ng of recombinant ATR protein was incubated with either 1 μg of MBP or MBP-SOG1 protein in the presence of [γ-^{32}P]ATP, after which samples were separated by SDS-PAGE and analyzed by autoradiography.

(D) Bacterially produced MBP-SOG1 protein was tested for its capability to physically interact with the promoter of one of SOG1's predicted targets, *BRCA1*. Approximately 50 ng of MBP or MBP-SOG1 was incubated with radiolabeled *BRCA1* promoter (−1 to −1500) using a standard EMSA approach. Analysis also included 50 ng of MBP-SOG1^{R155G} and MBP-SOG1^{S206F}, as well as MBP-SOG1 in the presence of increasing concentrations of unlabeled *BRCA1* promoter. Following separation of samples using an agarose gel, results were examined using autoradiography.

of capability to associate with target promoters. This would be consistent with the previous report that *sog1-1* mutants fail to induce a suite of genes, including *BRCA1*, following treatment with γ-radiation (Yoshiyama et al., 2009).

Al Promotes Expression of a Group of DNA Damage-Related SOG1-Regulated Genes

While Al treatment has been associated with upregulation of a large group of genes in multiple model systems (Chandran et al., 2008; Kumari et al., 2008), it has been difficult to identify which members of these Al-inducible groups are of primary relevance to Al toxicity and response. Therefore, demonstration that SOG1 is responsible at least in part for stoppage of root growth following chronic exposure to Al is expected to allow for determination of which Al-inducible genes are central to Al-dependent terminal differentiation. With this in mind, it was of interest to determine whether Al results in similar SOG1-dependent changes in gene expression as seen with γ-radiation (Yoshiyama et al., 2009). Several genes have been found to be substantially upregulated following exposure to γ-radiation, including many that are involved in response to and repair of damaged DNA. Examples include *BRCA1*, *PARP2*, *XRI1*, *RAD50*, and *RAD51*, along with a number of genes whose functions in relation to DNA damage response have yet to be elucidated (Yoshiyama et al., 2009).

In order to determine whether Al causes changes in expression of these SOG1-regulated genes, it was first necessary to determine the conditions that would allow for the best capture of these changes. This was particularly problematic since SOG1 does not persist after Al-dependent terminal differentiation (Figure 4B), making it necessary to determine at which point damage had accumulated to a high enough level to promote entrance into endoreduplication but not late enough to where the transition had already been initiated. For this work, *SOG1:GUS* expression in the root tip was followed over a time course of Al exposure. Col-0 wild-type transgenic plants expressing *SOG1:GUS* were grown in the presence of 1.50 mM $AlCl_3$ (pH 4.2) in a soaked gel environment, and samples were taken on successive days for visualization of GUS activity. As shown in Figure 5A, whereas GUS activity persisted in

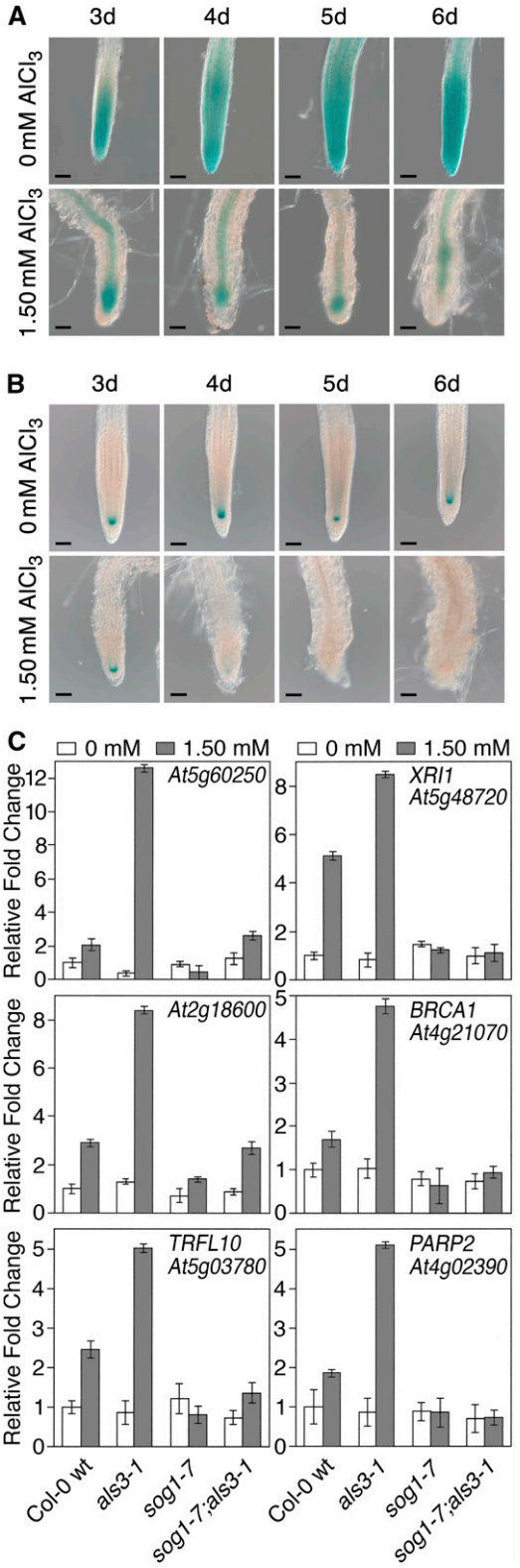

Figure 5. *SOG1* Is Required for Al-Dependent Induction of DNA Damage Response Genes.

(A) Seedlings of a *SOG1:GUS* transgenic line were grown in the absence or presence of 1.50 mM $AlCl_3$ (pH 4.2) in a soaked gel environment, after which roots were stained for 1 h for GUS activity on successive days. Bars = 50 μm.
(B) Seedlings of a *QC46:GUS* transgenic line were grown in the absence or presence of 1.50 mM $AlCl_3$ (pH 4.2) in a soaked gel environment, after which roots were stained for 24 h for GUS activity on successive days. Bars = 50 μM.
(C) Seedlings of Col-0 wild type, *als3-1*, *sog1-7*, and *sog1-7 als3-1* were grown for 3 d in the presence of either 0 or 1.50 mM $AlCl_3$ (pH4.2), after which tissue was harvested for RNA isolation. Following cDNA synthesis, real-time PCR for previously described SOG1-regulated transcriptional targets was performed (Yoshiyama et al., 2009). Mean ± SD values were determined from three technical replicates.

the root tip throughout the course of the experiment for untreated samples, growth of roots in the presence of Al resulted in a progressive loss of GUS activity starting 3 d after planting. It was also necessary to assess the status of the root QC on a daily basis through the use of the *QC46* reporter line. As shown in Figure 5B, consistent with the loss of SOG1:GUS activity, the root QC disappeared almost universally by day 5 of growth in the presence of 1.50 mM $AlCl_3$ (pH 4.2) in a soaked gel environment with a substantial decrease in GUS activity occurring between days 3 and 4. When considered together, these results suggest that the transition from an actively growing root tip to one that has transitioned to endoreduplication occurs between days 3 and 4 of chronic Al exposure, indicating that SOG1-dependent increases in gene expression in response to Al would be most likely observed within this window.

Because of this, seedling tissue was collected after 3 d of exposure to Al to assess whether Al causes upregulation of genes in a similar SOG1-dependent manner as seen for γ-radiation. For this experiment, Col-0 wild-type, *als3-1*, *sog1-7*, and *sog1-7 als3-1* seedlings were grown in the absence or presence of 1.50 mM $AlCl_3$ (pH 4.2) in a soaked gel environment for 3 d, after which whole seedlings were harvested for isolation of total RNA, cDNA synthesis, and subsequent RT-PCR analysis. As shown in Figure 5C, several genes that have been found to be highly induced by γ-radiation in a SOG1-dependent manner were used to perform a survey with regard to Al response (see also Supplemental Figure 1). Genes tested included those encoding a Zn finger of unknown function (*At5g60250*), a protein with an unknown role in DNA damage repair (*XRI1*), a putative ubiquitin conjugating enzyme (*At2g18600*), a putative telomere maintenance protein (*TRFL10*), an ortholog of the human breast cancer susceptibility gene (*BRCA1*), and a key component of microhomology-mediated DNA repair (*PARP2*). In each case, treatment with Al resulted in a measurable increase in expression in Col-0 wild type compared with no Al; the expression of these genes also increased significantly, even in comparison to Col-0 wild type, in Al-treated *als3-1* seedlings, consistent with the extreme Al hypersensitivity seen for this mutant. In contrast, expression of these genes was almost completely eliminated both for *sog1-7* and *sog1-7 als3-1* roots in comparison to the respective controls, thus indicating that Al triggers a SOG1-dependent transcriptional program that is similar to that observed following treatment with γ-radiation.

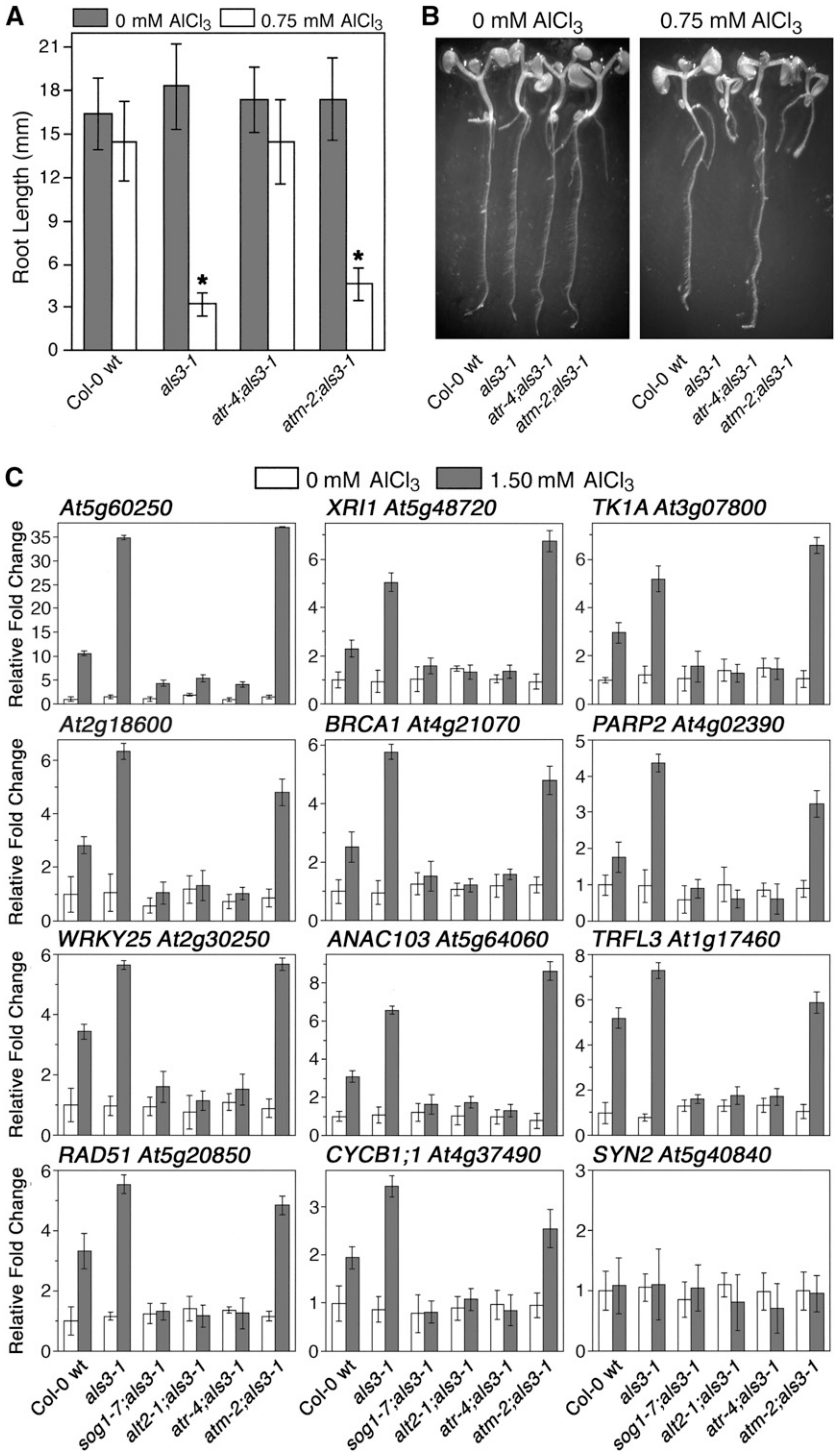

Figure 6. Response to Al in Arabidopsis Is an ATR-, ALT2-, and SOG1-Mediated Event Largely Independent of ATM.

(A) Col-0 wild type, *als3-1*, *atr-4 als3-1*, and *atm-2;als3-1* seedlings were grown for 7 d in the absence or presence of increasing amounts of $AlCl_3$ in a soaked gel environment (pH 4.2), following which root lengths were determined. Mean ± SD values were determined from 30 seedlings. Asterisk indicates significance at $P \leq 0.01$ when comparing Al-treated lines using the Tukey HSD test.

(B) Photos show representative control and Al-treated seedlings from each line.

(C) Seedlings of Col-0 wild type, *als3-1*, *sog1-7 als3-1*, *alt2-1 als3-1*, *atr-4 als3-1*, and *atm-2 als3-1* were grown in the absence or presence of 1.50 mM $AlCl_3$ (pH 4.2) in a soaked gel environment for 3 d, after which tissue was collected for RNA isolation. Following cDNA synthesis, real-time PCR was performed to

Al-Dependent Induction of DNA Damage Response Genes Does Not Require ATM

Since SOG1 has been demonstrated previously to function downstream of ATM in response to γ-radiation (Yoshiyama et al., 2013), we tested whether Al-responsive stoppage of root growth also required ATM. For this experimental approach, the capability of the *atm-2* loss-of-function mutation to suppress the Al hypersensitivity of *als3-1* was compared with that of *atr-4* (see Supplemental Figure 2 for *atm-2* genotype confirmation). Seedlings of Col-0 wild type, *als3-1*, *atr-4 als3-1*, and *atm-2 als3-1* were grown for 7 d in the absence or presence of 0.75 mM $AlCl_3$ (pH 4.2) in a soaked gel environment. As shown in Figures 6A and 6B, exposure to Al resulted in severe Al hypersensitivity in *als3-1* roots compared with Col-0 wild type, whereas *atr-4 als3-1* mutant roots were indistinguishable from Col-0 wild type in the presence of Al. In contrast, Al-treated roots of *atm-2 als3-1* were only marginally longer than those of *als3-1*, with both displaying the same terminal differentiation phenotype following Al exposure.

Because there is a clear discrepancy regarding the roles of ATR and ATM in mediating stoppage of root growth following exposure to Al, it was determined whether loss-of-function mutations for each had an impact on SOG1-dependent expression of genes following Al exposure. For this analysis, Col-0 wild type, *als3-1*, *sog1-7 als3-1*, *alt2-1 als3-1*, *atr-4 als3-1*, and *atm-2 als3-1* were grown for 3 d in the absence or presence of 1.50 mM $AlCl_3$ (pH 4.2) in a soaked gel environment, after which tissue was collected for RNA isolation, cDNA synthesis, and RT-PCR. As shown in Figure 6C, treatment with Al resulted in the same patterns of induction compared with γ-radiation for all genes tested for Col-0 wild type and *als3-1* with the exception of *SYN2* (*RAD21*), which encodes a key sister chromatid cohesion protein that is inducible with γ-radiation but not Al (Dong et al., 2001). In contrast, there was no apparent induction of any of these *SOG1*-regulated genes in *sog1-7 als3-1*, *alt2-1 als3-1*, or *atr-4 als3-1*, thus indicating that Al tolerance in each is correlated with failure to trigger the SOG1-dependent increase in expression of these genes following Al exposure. Loss of expression of this subset of genes was not observed for Al-treated *atm-2 als3-1*, which had clear induction of all SOG1-dependent Al-responsive genes to a level that was comparable to *als3-1*.

Loss-of-function mutations for both *BRCA1* (Block-Schmidt et al., 2011) and *PARP2* (Jia et al., 2013), which are Al-inducible SOG1 targets, were tested for their capability to grow in the presence of $AlCl_3$ in a soaked gel environment (pH 4.2). As shown in Figure 7A, two independent *brca1* loss-of-function mutants were modestly sensitive to a range of Al concentrations compared with Col-0 wild type, suggesting that BRCA1 plays a role in repair of Al-dependent DNA damage rather than transition of the root tip to endoreduplication. PARP2, in conjunction with PARP1, is a key component of microhomology-mediated end joining, which is one type of nonhomologous end joining (NHEJ) DNA repair mechanism that is related to base excision and single strand break repair (Jia et al., 2013). As shown in Figure 7B, loss of these two key components of microhomology-mediated end joining results in increased sensitivity to Al, consistent with Al acting as a DNA damage agent. Al hypersensitivity was even more pronounced for a *parp1 parp2 ku80* triple loss-of-function mutant, which represents a severe reduction in capability to carry out both classical NHEJ (KU80-related) and alternative NHEJ (PARP1- and PARP2-related) (Jia et al., 2013). These results suggest that Al has substantive negative effects on DNA integrity that in part requires ATR and SOG1-dependent induction of *BRCA1* and *PARP2* to repair the damage.

DISCUSSION

Aluminum toxicity is a critical worldwide problem that is a significant limitation to agriculture, especially in developing regions that have acid soil environments (von Uexkull and Mutert, 1995). While a great amount of attention has been paid to Al resistance mechanisms that rely on Al exclusion, little is known about the toxic consequences of internalized Al or the mechanisms that plants use to tolerate it. In recent years, factors predicted to be responsible for the uptake and redistribution of Al have been identified in part through mutagenesis screens that identified Al hypersensitive mutants. By using the Al-sensitive mutant *als3-1* to screen for suppressors, previous work identified two separate mutants with increased Al tolerance, with both of these affecting cell cycle checkpoints that arrest root growth in response to DNA damage agents (Rounds and Larsen, 2008; Nezames et al., 2012).

Identification of factors that have clear roles in DNA damage response suggests that a primary effect of Al toxicity is directly related to compromised genomic integrity, with Al possibly serving as a genotoxic agent, whether real or perceived. The latter argument is included based on the conundrum presented by the particular loss-of-function mutants previously identified, *atr-4* and *alt2-1*. Both *atr-4* and *alt2-1* mutations affect cell cycle checkpoints that are absolutely required for growth following exposure to various DNA damage agents, with loss of either leading to extreme sensitivity to agents such as γ-radiation, hydroxyurea, and/or cross-linking agents. It is curious that at the same time, loss of either cell cycle checkpoint results in increased tolerance to Al, suggesting that Al either is inappropriately perceived as a genotoxic agent by ATR and ALT2 or that ATR and ALT2 are so finely tuned that even the limited amount of genomic damage that might occur with Al could activate these factors yet in reality be relatively inconsequential to growth.

Clearly, cell cycle checkpoints are emerging as key regulators of Al responses, indicating that Al-dependent activation of these factors is central to terminal differentiation following chronic exposure to Al. This is further supported by demonstration that SOG1 is also required for root growth inhibition following Al treatment, as shown by isolation of a loss-of-function *sog1* mutant

Figure 6. (continued).

examine expression patterns for a group of previously documented SOG1-regulated genes (Yoshiyama et al., 2009). Mean ± SD values were determined from three technical replicates.

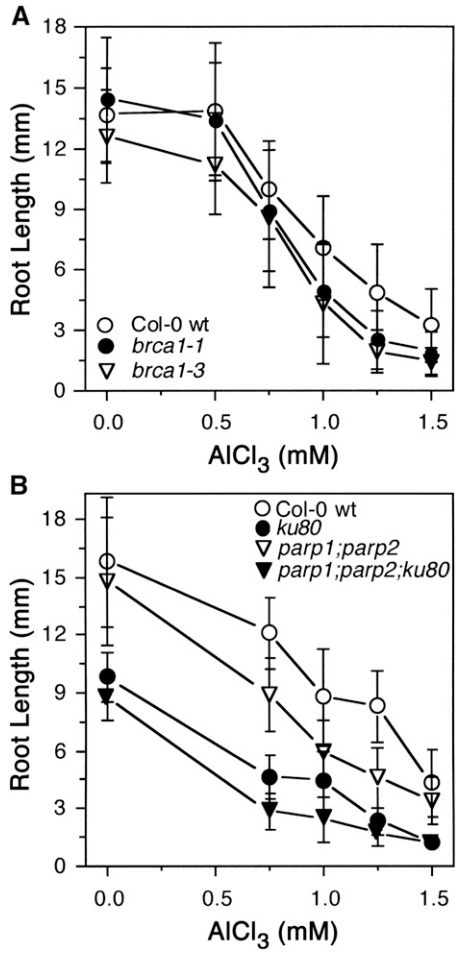

Figure 7. Roots of *brca1* and *parp2* Loss-of-Function Mutants Are Hypersensitive to Al.

(A) Two different T-DNA loss-of-function alleles of *BRCA1* were grown with Col-0 wild type in the absence or presence of increasing concentrations of $AlCl_3$ in a soaked gel environment (pH 4.2) for 7 d, after which root lengths were measured. Mean ± SD values were determined from 30 seedlings.
(B) Seedlings of Col-0 wild type and loss-of-function mutants representing key components of either C-NHEJ (*ku80*) or B-NHEJ (*parp1 parp2*) were grown for 7 d in the absence or presence of increasing concentrations of $AlCl_3$ in a soaked gel environment (pH 4.2), after which root lengths were measured. Mean ± SD values were determined from 30 seedlings.

from our *als3-1* suppressor screen. *SOG1* encodes a NAC family transcription factor argued to function analogously to mammalian p53 to upregulate a suite of DNA damage response genes (Yoshiyama et al., 2009). SOG1 was originally identified through a suppressor screen of the *uvh1* mutant, which affects a DNA endonuclease required for repair following exposure to UV and γ-radiation (Liu et al., 2000). This and subsequent work showed that a group of genes related to DNA repair are expressed in a SOG1- and ATM-dependent manner following γ-radiation, forcing transition of meristematic tissue into an endoreduplication program (Yoshiyama et al., 2009, 2013). Loss of *SOG1*, which is a phosphorylation target of ATM, results in failure to increase expression of genes such as *BRCA1* and *CYCB1;1*, thus preventing endoreduplication. At present, it is not known which of the transcriptional targets of SOG1 are determinants of entry into endocycling following exposure to γ-radiation since most of the members of this suite of genes encode factors required for DNA repair.

Demonstration that SOG1 is a critical component of Al-dependent terminal differentiation provides an important link between the DNA damage detection machinery and transcription in response to Al. Unlike γ-radiation stress, this stoppage of root

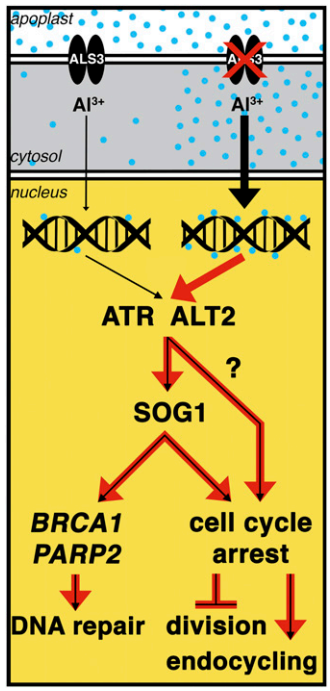

Figure 8. Model for Al-Dependent Stoppage of Root Growth.

Based on our results from identification of *als3-1* suppressors that increase Al tolerance, it is expected that Al acts as a genotoxic agent that in an unknown manner activates an ATR- and ALT2-dependent cell cycle checkpoint pathway to stop cell division following chronic Al exposure. Loss of *ALS3* function is predicted to result in increased Al accumulation in root tip cells that likely would lead to greater impacts on DNA and consequently cause hyperactivation of the ATR- and ALT2-dependent response pathway (red arrows within the nucleus). At present, it is not clear what role the WD-40 protein ALT2 plays in this active process, although it could be argued that ALT2 functions analogously to other WD-40 proteins involved in the mammalian DNA damage detection pathways of GGNER and TCNER. Regardless, both ATR and ALT2, but not ATM, function to halt cell division, trigger QC differentiation, and promote endocycling at least in part through SOG1. This includes promotion of a transcriptional response to Al that is composed of a suite of genes that are related to two distinctly different functions. One set, as demonstrated by analyses of loss-of-function mutants for *BRCA1* and *PARP2*, encodes products that are responsible for repair of the apparently limited DNA damage that occurs following treatment with Al. The other set, while still cryptic with regard to its members, represents factors that are responsible for transitioning from actively dividing root cells to terminal differentiation and endoreduplication following Al treatment. It could be argued that increased Al tolerance occurs following mutational loss of these cell cycle checkpoints because the negative consequences of cell cycle arrest far outweigh the actual genotoxic consequences of Al.

growth is ATM independent (Figures 6A and B), indicating that at least in respect to Al stress, SOG1 functions downstream of ATR rather than ATM. This is of particular importance since it is suggestive of the type of damage that ATR and SOG1 are detecting in the context of Al. Interestingly, there are clear transcriptional differences between Al treatment and exposure to γ-radiation, most notably in the form of *RAD21* (Figure 6C), suggesting that each DNA stress results in a unique transcriptional fingerprint that may be informative in relation to their respective impacts on genomic integrity. Unlike exposure to γ-radiation, none of these SOG1-dependent transcripts are inducible in an ATM-dependent manner following Al treatment, yet all require functional ATR and ALT2 (Figure 6C). This indicates that ATR, ALT2, and SOG1 form an Al-response pathway that largely does not require ATM.

This relationship between ATR and SOG1 is likely direct, since as with ATM in γ-radiation (Yoshiyama et al., 2013), ATR is capable of phosphorylating SOG1 in vitro (Figure 4C). When combined with the observation that both ATR and SOG1 regulate expression of these genes, it could be argued that the phosphorylation-dependent relationship between ATR and SOG1 is a key step in translation of Al-dependent damage into cell cycle arrest and terminal differentiation. Unfortunately, as with γ-radiation, it is not clear which members of this suite of genes are responsible for triggering an Al-treated root to switch from active cell division to one that forces the root tip to differentiate its QC and initiate endoreduplication. This certainly bears further investigation since as of now, analysis of loss-of-function mutants for the SOG1-inducible genes that can be maintained as homozygotes did not result in demonstration of Al tolerance, but rather in most cases mild to moderate Al sensitivity (e.g., *BRCA1* and *PARP2*) (Figure 7).

From our results, a model for stoppage of root growth following chronic exposure to Al can be developed (Figure 8). In this model, Al impacts DNA in a currently unknown way, possibly in an electrostatic manner. Such an interaction may cause a conformational change reminiscent of covalent cross-linkers such as Mitomycin C and cisplatin since Al^{3+} is expected to have high affinity for the negatively charged phosphodiester DNA backbone (Karlik et al., 1980) and would interact with this backbone differently than divalent cations (Nezames et al., 2012). Interestingly, ATR, ALT2, and SOG1 all respond to DNA cross-linking agents and are linked to Al-dependent stoppage of root growth (Rounds and Larsen, 2008; Nezames et al., 2012; Hu et al., 2015). One could predict that such an interaction would hold DNA in a conformation that negatively impacts replication fork progression, potentially through inhibition of unwinding of genomic DNA since Al^{3+} may raise the T_m of the double helix (Latha et al., 2002). Regardless of the physical consequences of Al on DNA structure or integrity, the predicted genotoxic effects of Al are clearly sufficient to activate an ATR- and ALT2-dependent cell cycle checkpoint mechanism, as demonstrated by the increase in Al tolerance seen for the respective loss-of-function mutants. This ATM-independent mechanism functions at least in part through SOG1 to promote transcription of a group of genes. A subset of these genes is predicted to be related in some unknown manner to a mechanism that forces a programmatic change in the root tip and QC, triggering this tissue to switch to endoreduplication and causing terminal differentiation and permanent stoppage of growth of the primary root. While significant work remains to be done, including determining the genotoxic consequences of Al that activate this ATR-regulated pathway and developing an understanding of how certain SOG1 transcriptional targets halt root growth following Al treatment, it is clear that terminal differentiation of the root tip following chronic exposure to Al is an active event mediated by cell cycle checkpoint factors.

METHODS

Plant Growth Conditions

Experiments using Al-soaked gel and Al-containing hydroponics were conducted on common plates as previously described (Larsen et al., 1996, 2005). For all seedling growth experiments, Col-0 wild type and mutant *Arabidopsis thaliana* seeds were surface-sterilized and cold stratified at 4°C for 4 d in the dark to synchronize germination. Seeds were then sown on either soaked gel plates or hydroponic plates. For soaked gel plates, nutrient medium (pH 4.2) consisted of 80 mL of 1 mM KNO_3, 0.2 mM KH_2PO_4, 2 mM $MgSO_4$, 0.25 mM $(NH_4)_2SO_4$, 1 mM $Ca(NO_3)_2$, 1 mM $CaSO_4$, 1 mM K_2SO_4, 1 μM $MnSO_4$, 5 μM H_3BO_3, 0.05 μM $CuSO_4$, 0.2 μM $ZnSO_4$, 0.02 μM $NaMoO_4$, 0.1 μM $CaCl_2$, 0.001 μM $CoCl_2$, 1% sucrose, and 0.125% Gellan gum (Gell-8Gro; ICN Biomedicals). For Al experiments, the solidified nutrient medium was soaked with 20 mL of nutrient medium ± $AlCl_3$ (pH 4.2) for 2 d, after which the soaking solution was removed and seeds were planted and allowed to grow for 7 d unless otherwise specified. For dose-response analyses in a hydroponic environment, seedlings were grown on 250-μm mesh polypropylene screen in 100 × 15-mm X-plate dishes with 40 mL of liquid nutrient medium (pH 4.2) described above with varying concentrations of $AlCl_3$. All growth analyses were performed in a Percival 136LLVL plant growth chamber (Percival Scientific) with light intensity at 40 μmol of photons/s/m^2 under a 24-h light cycle at 20°C.

Phenotypic Assessment of *sog1-7 als3-1*

RNA gel blot analyses and assessment of callose deposition were performed as previously described (Gabrielson et al., 2006). For ICP-OES analysis, roots of 6-d-old wild-type, *als3-1*, and *sog1-7 als3-1* plants that were grown hydroponically were treated with 50 μM $AlCl_3$ (pH 4.2) for 2 d, after which roots were washed with nutrient medium without $AlCl_3$. Subsequently, the distal 25% (~3 to 4 mm) of sample roots was harvested, dried, and ashed in pure nitric acid. Samples were resuspended in 5 mL of 1% nitric acid and analyzed using a Perkin-Elmer Optima 3000 DV ICP-OES.

Map-Based Cloning

Genomic DNA isolation and PCR-based mapping were performed as described previously (Larsen et al., 2005). For mapping, a new cleaved-amplified polymorphic sequence marker was generated for *At1g25570* (5′ forward GTGAACAATAATGTGTATGCTAC and 3′ reverse GTCGTTG-ATGCTACTGGAAATG), with digestion by αTaq1 giving two bands for Col-0 wild type and one band for La-0 wild type. Candidate genes from this narrow region on chromosome 1 were amplified by PCR and sequenced by the ICBR at the University of Florida, Gainesville. Sequences were compared with the published *Arabidopsis* genome to identify potential mutations, with putative mutations resequenced for verification. In order to follow the *sog1-7* mutation in genetic crosses, a cleaved-amplified polymorphic sequence marker was generated for *At1g25580* (Supplemental Table 1). Digestion of the PCR product with *Dde*I resulted in two bands for Col-0 wild type and one band for *sog1-7*. More information on *sog1-7* and other mutants found in this article can be found in Supplemental Table 2.

GUS Staining

All GUS staining experiments were conducted as previously described (Rounds and Larsen, 2008), with microscopy performed using a Leica DMR

differential interference contrast light microscope. Seedlings were grown on soaked gel media for 7 d, unless otherwise specified, collected, and subsequently fixed in 5 mL 90% acetone on ice for 20 to 30 min. Acetone was removed and seedlings were rinsed in 5 mL of rinse solution [50 mM $NaPO_4$, 0.5 mM $K_3Fe(CN)_6$, and 0.5 mM $K_4Fe(CN)_6$]. Rinse solution was removed and seedlings were treated with 5 mL GUS stain [50 mM $NaPO_4$, 0.5 mM $K_3Fe(CN)_6$, 0.5 mM $K_4Fe(CN)_6$, and 2 mM X-Gluc (Gold Biotechnology G1281C)], vacuum infiltrated for 5 min at room temperature, and incubated at 37°C for noted times. Stain solution was removed and seedlings were stored in 70% ethanol until analyzed using differential interference contrast microscopy. For CYCB1;1 GUS analyses, 60 total seedlings from each line and each treatment were scored for level of blue color at the root tip after 1 h staining for GUS activity.

Confocal Microscopy

For estimation of nucleus size, seedlings were fixed in FAA under vacuum for 2 h, washed two times in PBS, stained in 1 μg/mL DAPI overnight at 4°C, and stored in PBS. Stained root tips were viewed using a Leica SP2 confocal laser microscope at 40× magnification with excitation at 360 nm and emission at 460 nm.

MBP-SOG1 Fusion Protein Production

A cDNA for the full CDS of SOG1 was generated by PCR with *PfuTurbo Taq* DNA polymerase (Agilent Technologies), cloned into *pGEM-T EZ* (Promega), and sequenced. After transferring into the *pMAL-C2* expression vector with *Xmn*I and *Xba*I (New England Biolabs), the *MBP-SOG1* construct was transformed into BL21(DE3)-competent *Escherichia coli* (New England Biolabs) after which protein was produced following induction for 3 h with 0.4 mM isopropyl β-D-1-thiogalactopyranoside. MBP-SOG1 was isolated by sonication followed by purification with amylose resin (New England Biolabs) and then elution with 50 mM maltose. In order to generate the mutant forms of MBP-SOG1, *SOG1* in the *pMAL-C2* vector was mutagenized using the QuikChange II mutagenesis kit (Agilent Technologies) after which candidates were sequenced. Mutant forms were subsequently produced in the same manner as wild-type MBP-SOG1.

In Vitro ATR Kinase Assay

A cDNA representing the full CDS of ATR was amplified by PCR with *PfuTurbo* Taq DNA polymerase, cloned into *pGEM-T EZ*, sequenced, and then transferred to the *pAcGHLT-B* (BD Biosciences) baculovirus vector with *Not*I (primer sequences can be found in Supplemental Table 1). Recombinant baculovirus was generated according to the manufacturer's instructions, after which GST-ATR protein was produced by infection of *Sf9* insect cells. Proteins were purified per the manufacturer's instructions, including use of insect cell lysis buffer and glutathione agarose beads to produce a GST-ATR fusion protein.

For the ATR kinase assay, 50 ng of GST-ATR was incubated in vitro with 1 μg of either MBP or MBP-SOG1 produced in BL21(DE3) *E. coli* cells. Reaction buffer was composed of 10 mM HEPES (pH 7.5), 50 mM NaCl, 10 mM $MgCl_2$, 1 mM DTT, 0.5 mM Na_3VO_4, 10 μM ATP, and 20 μCi of [γ-^{32}P] ATP (3000 Ci/mmol). Reactions were incubated for 30 min at 20°C, after which samples were separated by SDS-PAGE, dried, and visualized by autoradiography.

EMSA Conditions

For gel-shift analysis, the *BRCA1* promoter (−1 to −1500) was generated by PCR with *PfuTurbo* Taq DNA polymerase, cloned into *pGEM-T EZ*, and sequenced. The promoter (10 pmoles) was isolated by *Eco*RI digestion, dephosphorylated by Calf Intestinal Alkaline Phosphatase (Promega), and subsequently radiolabeled with [γ-^{32}P]ATP using T4 polynucleotide kinase (Promega) following the manufacturer's instructions. For each association, 20 fmoles of the radiolabeled probe was incubated with 50 ng of MBP, MBP-SOG1, MBP-SOG1^{R155G}, or MBP-SOG1^{S206F} on ice using the Thermo Scientific EMSA kit following manufacturer's instructions. Samples were separated using a 1% agarose gel, dried, and visualized by autoradiography. For competition analysis, EMSA conditions were the same with the exception that increasing amounts of unlabeled *BRCA1* promoter (−1 to −1500) were added to the gel shift reaction with MBP-SOG1.

Real-Time PCR Analysis

For real-time PCR analysis, seedlings were grown in the absence or presence of 1.50 mM $AlCl_3$ (pH 4.2) in a soaked gel environment, after which tissue was collected for RNA extraction using Trizol (Invitrogen). RNA samples were DNase treated with RQ1 RNase-free DNase (Promega), and cDNA was generated using a SuperScript III kit (Invitrogen 18080-051) following the manufacturer's instructions. Real-time PCR reactions were performed according to Bio-Rad iQ SYBR Green Supermix instructions and run on the Bio-Rad iQ Real-time system under the following conditions: one repeat of 3 min at 95°C, followed by 40 repeats of 30 s at 95°C, 40 s at 55°C, and 45 s at 72°C, followed by a melt curve encompassing 80 steps of 0.5°C from 55 to 95°C. Fluorescence was measured during the 72°C extension step and at each step of the melt curve. Gene expression levels were calculated using the DDCt method as described in the Real-Time PCR Handbook (Thermo Fisher Scientific, 2014). Mean ± SD values were determined from three technical replicates, and the equations listed below were used for calculations. Arabidopsis *EF-1a* was used as the reference gene (Remans et al., 2008) because its expression was found to be Al independent for all genotypes considered (Supplemental Figure 3). Primer sequences for all genes used can be found in Supplemental Table 1. Replication efficiencies of RT-PCR primers were generated from standard curves produced from RT-PCR reactions as described above with 500, 100, 50, 10, 5, 1, 0.5, and 0.1 ng of Arabidopsis cDNA template. Log values of template quantity were graphed against the Ct values as determined from three technical replicates to generate a standard curve for each primer set, the slope, and R^2 values, from which were used to calculate reaction efficiencies (Supplemental Table 3). Only efficiencies between 95 and 105% and standard curve $R^2 > 0.98$ were accepted.

$$SD = \sqrt{\left(SD^2_{\text{reference gene}} + SD^2_{\text{Got}}\right)}$$

$$Ct_{\text{GOI (Col}-0,\ 0\ \text{mM)}} - Ct_{\text{reference gene (Col}-0,\ 0\ \text{mM)}} = DCt_{\text{CALIBRATOR}}$$

$$Ct_{\text{GOI (sample)}} - Ct_{\text{reference gene (sample)}} = DCt_{\text{SAMPLE}}$$

$$DCt_{\text{SAMPLE}} - DCt_{\text{CALIBRATOR}} = DDCt$$

$$\text{Relative Fold Change} = 2^{-DDCt}$$

$$E = 10^{-1/\text{slope from standard curve}}$$

$$\%\ \text{Efficiency} = (E-1)^{*}100$$

GOI is the gene of interest, DCt is the delta cycle threshold, DDCt is the delta delta cycle threshold, and E is the PCR efficiency.

Accession Numbers

Sequence data from this article can be found in the Arabidopsis Genome Initiative or GenBank/EMBL databases under the following accession numbers: *SOG1* (AT1G25580), *ALS3* (AT2G37330), *ATR* (AT5G40820),

ALT2 (AT4G29860), *ATM* (AT3G48190), *EF1a* (AT5G60390), *BRCA1* (AT4G21070), *GMI1* (AT5G24280), *RAD51* (AT5G20850), *TRFL10* (AT5G03780), *WRKY25* (AT2G30250), *TRFL3* (AT1G17460), *RAD17* (AT5G66130), *ANAC103* (AT5G64060), *XRI1* (AT5G48720), *TK1A* (AT3G07800), *CYCB1;1* (AT4G37490), *SYN2* (AT5G40840), *PARP2* (AT4G02390), *PARP1* (AT2G31320), *KU80* (AT1G48050), AT2G18600, AT2G45460, AT5G60250, and AT5G60390.

Supplemental Data

Supplemental Figure 1. Expression analysis of reference gene *EF1a*.

Supplemental Figure 2. Al-responsive expression of DNA damage response genes is largely independent of ATM.

Supplemental Figure 3. *atm-2* genotype analysis for generation of an *atm-2 als3-1* double mutant.

Supplemental Table 1. Primer sequences.

Supplemental Table 2. Replication efficiencies of RT PCR primers.

Supplemental Table 3. Mutant genotyping methods and sources.

ACKNOWLEDGMENTS

We thank Megan Rounds, Jesus Barajas, and Chinh Nguyen of the UCR Biological Sciences Department for technical assistance, Woody Smith and Chris Amrhein of the UCR Environmental Sciences Department for ICP-OES measurements, and Patricia Springer of the UCR Botany and Plant Sciences Department for use of microscopy equipment. We also thank Anne Britt of the University of California-Davis, Kaoru Yoshiyama of the Nara Institute of Science and Technology, Sylvia de Pater of Leiden University, and Holger Puchta and Oliver Trapp of the Karlsruhe Institute of Technology for providing seed stocks. This work was supported by the Physiological Mechanisms and Biomechanics Program of the National Science Foundation (award number 1119884) and the California Agriculture Experiment Station.

AUTHOR CONTRIBUTIONS

C.A.S., S.C.B., and P.B.L. all contributed to design and implementation of experiments, data analysis, and writing of the article.

Received February 23, 2015; revised August 4, 2015; accepted August 13, 2015; published August 28, 2015.

REFERENCES

Block-Schmidt, A.S., Dukowic-Schulze, S., Wanieck, K., Reidt, W., and Puchta, H. (2011). BRCC36A is epistatic to BRCA1 in DNA crosslink repair and homologous recombination in *Arabidopsis thaliana*. Nucleic Acids Res. **39:** 146–154.

Chandran, D., Sharopova, N., Ivashuta, S., Gantt, J.S., Vandenbosch, K.A., and Samac, D.A. (2008). Transcriptome profiling identified novel genes associated with aluminum toxicity, resistance and tolerance in *Medicago truncatula.* Planta **228:** 151–166.

Colón-Carmona, A., You, R., Haimovitch-Gal, T., and Doerner, P. (1999). Technical advance: spatio-temporal analysis of mitotic activity with a labile cyclin-GUS fusion protein. Plant J. **20:** 503–508.

Culligan, K., Tissier, A., and Britt, A. (2004). ATR regulates a G2-phase cell-cycle checkpoint in *Arabidopsis thaliana.* Plant Cell **16:** 1091–1104.

Culligan, K.M., Robertson, C.E., Foreman, J., Doerner, P., and Britt, A.B. (2006). ATR and ATM play both distinct and additive roles in response to ionizing radiation. Plant J. **48:** 947–961.

Dong, F., Cai, X., and Makaroff, C.A. (2001). Cloning and characterization of two Arabidopsis genes that belong to the RAD21/REC8 family of chromosome cohesin proteins. Gene **271:** 99–108.

Gabrielson, K.M., Cancel, J.D., Morua, L.F., and Larsen, P.B. (2006). Identification of dominant mutations that confer increased aluminium tolerance through mutagenesis of the Al-sensitive Arabidopsis mutant, *als3-1.* J. Exp. Bot. **57:** 943–951.

Hoekenga, O.A., et al. (2006). *AtALMT1*, which encodes a malate transporter, is identified as one of several genes critical for aluminum tolerance in Arabidopsis. Proc. Natl. Acad. Sci. USA **103:** 9738–9743.

Horst, W.J., Puschel, A.-K., and Schmohl, N. (1997). Induction of callose formation is a sensitive marker for genotypic aluminum sensitivity in maize. Plant Soil **192:** 23–30.

Horst, W.J., Wang, Y., and Eticha, D. (2010). The role of the root apoplast in aluminium-induced inhibition of root elongation and in aluminium resistance of plants: a review. Ann. Bot. (Lond.) **106:** 185–197.

Hu, Z., Cools, T., Kalhorzadeh, P., Heyman, J., and De Veylder, L. (2015). Deficiency of the Arabidopsis helicase RTEL1 triggers a SOG1-dependent replication checkpoint in response to DNA cross-links. Plant Cell **27:** 149–161.

Jia, Q., den Dulk-Ras, A., Shen, H., Hooykaas, P.J., and de Pater, S. (2013). Poly(ADP-ribose)polymerases are involved in microhomology mediated back-up non-homologous end joining in *Arabidopsis thaliana.* Plant Mol. Biol. **82:** 339–351.

Karlik, S.J., Eichhorn, G.L., Lewis, P.N., and Crapper, D.R. (1980). Interaction of aluminum species with deoxyribonucleic acid. Biochemistry **19:** 5991–5998.

Kochian, L.V. (1995). Cellular mechanisms of aluminum toxicity and resistance in plants. Annu. Rev. Plant Physiol. Plant Mol. Biol. **46:** 237–260.

Kumari, M., Taylor, G.J., and Deyholos, M.K. (2008). Transcriptomic responses to aluminum stress in roots of *Arabidopsis thaliana.* Mol. Genet. Genomics **279:** 339–357.

Larsen, P.B., Cancel, J., Rounds, M., and Ochoa, V. (2007). Arabidopsis *ALS1* encodes a root tip and stele localized half type ABC transporter required for root growth in an aluminum toxic environment. Planta **225:** 1447–1458.

Larsen, P.B., Geisler, M.J.B., Jones, C.A., Williams, K.M., and Cancel, J.D. (2005). *ALS3* encodes a phloem-localized ABC transporter-like protein that is required for aluminum tolerance in Arabidopsis. Plant J. **41:** 353–363.

Larsen, P.B., Kochian, L.V., and Howell, S.H. (1997). Al inhibits both shoot development and root growth in *als3*, an Al sensitive Arabidopsis mutant. Plant Physiol. **114:** 1207–1214.

Larsen, P.B., Tai, C.Y., Kochian, L.V., and Howell, S.H. (1996). Arabidopsis mutants with increased sensitivity to aluminum. Plant Physiol. **110:** 743–751.

Latha, K.S., Anitha, S., Rao, K.S.J., and Viswamitra, M.A. (2002). Molecular understanding of aluminum-induced topological changes in (CCG)12 triplet repeats: relevance to neurological disorders. Biochim. Biophys. Acta **1588:** 56–64.

Liu, Z., Hossain, G.S., Islas-Osuna, M.A., Mitchell, D.L., and Mount, D.W. (2000). Repair of UV damage in plants by nucleotide excision repair: Arabidopsis UVH1 DNA repair gene is a homolog of *Saccharomyces cerevisiae* Rad1. Plant J. **21:** 519–528.

Macdonald, T.L., and Martin, R.B. (1988). Aluminum ion in biological systems. Trends Biochem. Sci. **13:** 15–19.

Nezames, C.D., Sjogren, C.A., Barajas, J.F., and Larsen, P.B. (2012). The Arabidopsis cell cycle checkpoint regulators TANMEI/ALT2 and ATR

mediate the active process of aluminum-dependent root growth inhibition. Plant Cell **24:** 608–621.

Remans, T., Smeets, K., Opdenakker, K., Mathijsen, D., Vangronsveld, J., and Cuyper, A. (2008). Normalisation of real-time RT-PCR gene expression measurements in *Arabidopsis thaliana* exposed to increased metal concentrations. Planta **227:** 1343–1349.

Rounds, M.A., and Larsen, P.B. (2008). Aluminum dependent root growth inhibition results from AtATR dependent cell cycle arrest and loss of the quiescent center in Arabidopsis. Curr. Biol. **18:** 1495–1500.

Ryan, P.R., DiTomaso, J.M., and Kochian, L.V. (1993). Aluminum toxicity in roots: an investigation of spatial sensitivity and the role of the root cap. J. Exp. Bot. **44:** 437–446.

Sabatini, S., Heidstra, R., Wildwater, M., and Scheres, B. (2003). SCARECROW is involved in positioning the stem cell niche in the *Arabidopsis* root meristem. Genes Dev. **17:** 354–358.

Sasaki, T., Yamamoto, Y., Ezaki, B., Katsuhara, M., Ahn, S.J., Ryan, P.R., Delhaize, E., and Matsumoto, H. (2004). A wheat gene encoding an aluminum-activated malate transporter. Plant J. **37:** 645–653.

von Uexkull, H.R., and Mutert, E. (1995). Global extent, development and economic impact of acid soils. Plant Soil **171:** 1–15.

Yi, D., et al. (2014). The Arabidopsis SIAMESE-RELATED cyclin-dependent kinase inhibitors SMR5 and SMR7 regulate the DNA damage checkpoint in response to reactive oxygen species. Plant Cell **26:** 296–309.

Yoshiyama, K., Conklin, P.A., Huefner, N.D., and Britt, A.B. (2009). *Suppressor of gamma response 1* (*SOG1*) encodes a putative transcription factor governing multiple responses to DNA damage. Proc. Natl. Acad. Sci. USA **106:** 12843–12848.

Yoshiyama, K.O., Kobayashi, J., Ogita, N., Ueda, M., Kimura, S., Maki, H., and Umeda, M. (2013). ATM-mediated phosphorylation of SOG1 is essential for the DNA damage response in Arabidopsis. EMBO Rep. **14:** 817–822.